Available online at www.sciencedirect.com
ScienceDirect
Ceramics International 38 (2012) 981–985
CERAMICS INTERNATIONAL
www.elsevier.com/locate/ceramint

Temperature field and residual stress analysis of multilayer pyroelectric thin film

Zunping Xu [a,b], Dongxu Yan [a], Dingquan Xiao [a], Ping Yu [a], Jianguo Zhu [a,*]

[a] College of Materials Science and Engineering, Sichuan University, Chengdu 610064, China
[b] College of Materials Science and Engineering, Southwest University, Chongqing 400715, China

Received 8 July 2011; received in revised form 8 August 2011; accepted 10 August 2011
Available online 17 August 2011

Abstract

The two-dimensional finite element model was built for the multilayer pyroelectric thin film. The temperature field and residual stress were simulated. The results show that porous silica film as a thermal-insulation layer and a reasonable model structure are effective for decreasing the heat loss. The silicon substrate and pyroelectric thin film that influence the temperature variation rate in pyroelectric thin film are also discussed. The annealing temperature and model structure have significant influence on residual stresses of pyroelectric thin film. The residual stresses increase rapidly with the increase of annealing temperature. The scanning electron microscopy (SEM) is employed to investigate the morphology of the pyroelectric thin film. The results show that the pyroelectric thin film annealed at 750 °C has a crack structure.

Keywords: A. Films; D. $BaTiO_3$ and titanates; D. Perovskites

1. Introduction

In the past decades, much attention had been paid to the pyroelectric detection of infrared radiation (IR) due to the advantages offered by the pyroelectric detectors: room temperature operation, good sensitivity, and flat spectral response from near ultraviolet up to far infrared, etc. [1,2]. In order to minimize the heat loss caused by the vertical thermal conduction from the pyroelectric thin film to the substrate, and thus increase its pyroelectric response, various low thermal conductive materials and multilayer films have been used [3]. Generally, pyroelectric thin films used as pyroelectric detectors have lead-based and lead-free pyroelectric thin films. Compared with lead-based pyroelectric thin film [4,5], barium strontium titanate (BST) thin film is becoming one of the most interesting pyroelectric materials for uncooled infrared detectors due to its relatively high pyroelectric properties [6].

As we all know, dynamic pyroelectric response current of multilayer pyroelectric thin film IR detector can be expressed as [7]:

$$i_p = \frac{\eta\gamma A \mathrm{d}T}{\mathrm{d}t} \quad (1)$$

where η is the absorption coefficient of radiation, γ is the pyroelectric coefficient of pyroelectric thin film, A is the detector area, and $\mathrm{d}T/\mathrm{d}t$ is the temperature variation rate of pyroelectric film. The response current of multilayer pyroelectric thin film is in proportion to the temperature variation rate of the pyroelectric film.

The internal residual stress (which is mainly induced by thermal and misfit strain) has a great impact on the dielectric and ferroelectric properties of BST thin films. The BST thin films possess high dielectric constant [8] and excellent ferroelectric property [9] when the BST thin films possess low residual stress. Stress is one of the critical parameters for designing the dielectric properties, especially for heteroepitaxial thin films two-dimensionally clamped by the underlying substrate lattice.

However, there have been few systematic reports on the temperature variation rate and residual stress of BST thin film by using the finite element method (FEM), which are important not only for current practical applications, but also for basic studies into the nature of ferroelectric thin films.

Using FEM to solve complex thermal and mechanical problems is an extremely powerful and flexible approach. Many non-linear aspects of behavior can be accounted for where an exact analytical solution is impossible. Li et al. [7] use the finite element method to simulate the temperature field of multilayer PZT pyroelectric thin film, Zheng et al. [10]

* Corresponding author. Tel.: +86 028 85412415; fax: +86 028 85416050.
E-mail address: nic0400@scu.edu.cn (J. Zhu).

0272-8842/$36.00
doi:10.1016/j.ceramint.2011.08.019

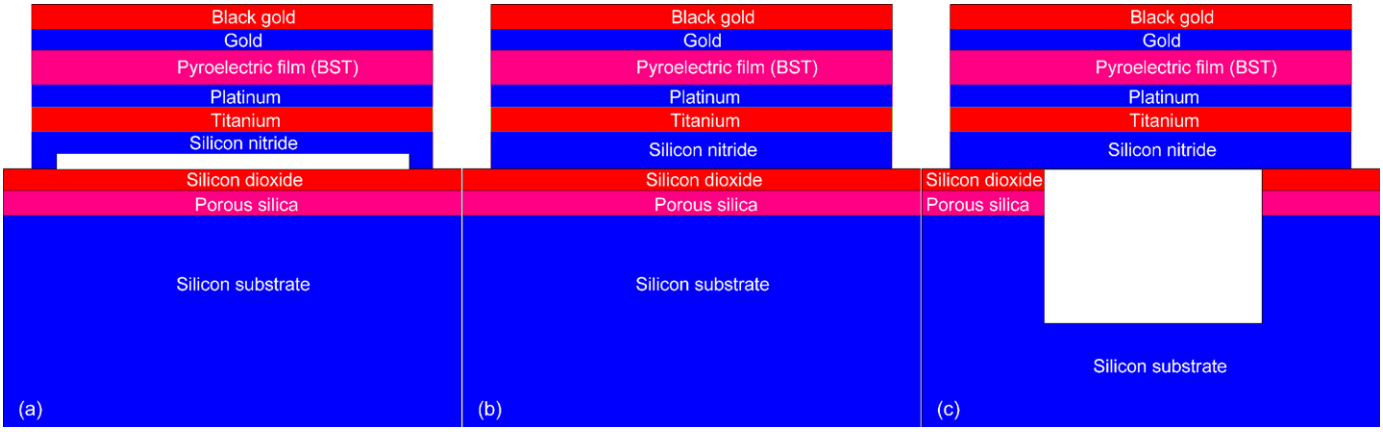

Fig. 1. Different model structures: (a) MBS, (b) CFS and (c) TS.

calculated Young's modulus of nanobelt using FEM and Liu et al. [11] investigated the residual stress fields of cold expansion hole by the FEM.

In this study, three different model structures including micro-bridge structure (MBS), tunnel structure (TS) and composite film structure (CFS) have been created to study the temperature field and thermal residual stress of multilayer BST thin films by the FEM. The effect of BST film, silicon substrate and porous silica on the temperature field, and the effect of annealing temperature on the thermal residual stress are considered. The morphology of the pyroelectric film was investigated by SEM. The cross-section of different models is shown in Fig. 1.

2. Finite element models

The geometry of model is symmetrical, therefore only one half of finite element model is established. Symmetry boundary conditions were used at the symmetric lines. Fig. 2 shows the finite element model of MBS. The values of parameters for calculation are summarized in Table 1. The properties were assumed to be similar to those of the bulk material values. For modeling, it was assumed that the properties were isotropic.

The thermal stress of the BST thin film can be determined from Eq. (2) [15],

$$\sigma_f = \frac{E_{ef}\int_{T_r}^{T_d}(\alpha_s - \alpha_f)dT}{1 + 4(E_{ef}/E_{es})(h/H)} \quad (2)$$

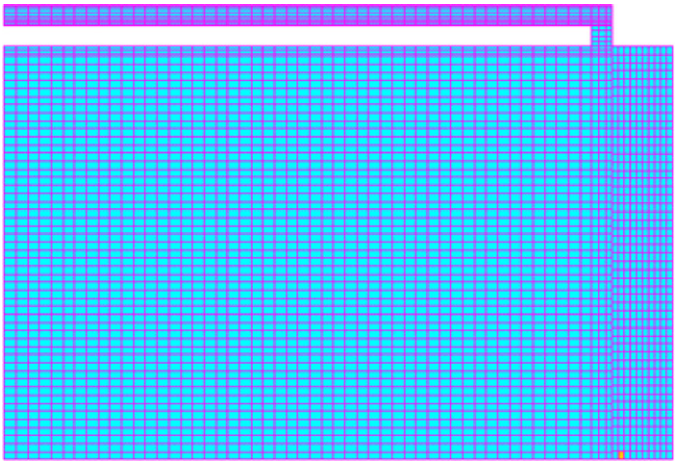

Fig. 2. FEM model.

where $E_{ef} = E_f/(1-\nu_f)$, $E_{es} = E_s/(1-\nu_s)$, E_f, E_s, ν_f, ν_s, h, H, α_f, α_s represent the effective elastic modulus, elastic modulus, Poisson's ratio, thickness and thermal expansion coefficient of film and substrate, respectively, T_d and T_r represent substrate temperature and room temperature, respectively.

Fig. 3 shows the model including only one-layered BST thin film and silicon substrate. In order to test the finite element model, we calculated the model according to Eq. (1) and simulated the model by FEM. The results are shown in Fig. 4. From Fig. 4, we can see that the results of FEM agree well with

Table 1
Parameters used in simulation [3,7,12–14].

Material	Thermal conductivity ($W\ m^{-1}\ K^{-1}$)	Specific heat ($J\ kg^{-1}\ K^{-1}$)	Density ($kg\ m^{-3}$)	Elastic modulus (GPa)	Poisson's ratio	Thermal expansion coefficient ($\times 10^{-6}\ K^{-1}$)	Thickness (μm)
Si	145	708	2330	130	0.23	2.6	~400
Porous silica	0.02	780	1320				~10
SiO_2	1.4	780	2202	78	0.17	0.55	0.5
Si_3N_4	17	700	3184	220	0.27	0.8	0.5
Ti	20.5	527	4500	78	0.38	10.8	0.05
Pt	69.5	133	21 450	276	0.39	9	0.1
BST	6.2	420	6020	230	0.25	10.5	~1
Au	300	127	19 320	108	0.3	14.2	0.1
Black gold	2	130	345				0.05

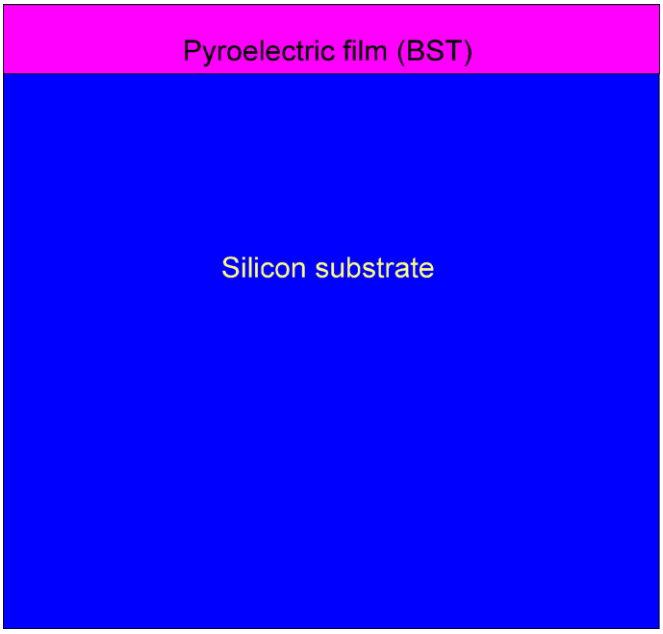

Fig. 3. One-layered BST film model.

the theoretical results. It shows that the finite element model is reasonable.

The incident radiation power P to the detector can be determined from Eq. (3) [7],

$$P = \alpha \frac{\sigma(\varepsilon T^4 - \varepsilon_0 T_0^4)A}{\pi L^2} \quad (3)$$

where α is the modulation factor of chopper, σ is the Boltzmann's constant, ε is the emissivity of black body, ε_0 is the emissivity of chopper, T is the temperature of black body, T_0 is the ambient temperature (293 K), A is the aperture of the diaphragm, and L is the distance from the black body to the detector. So, the incident radiation power to the detector is about 1.23×10^{-12} W μ m^{-2}.

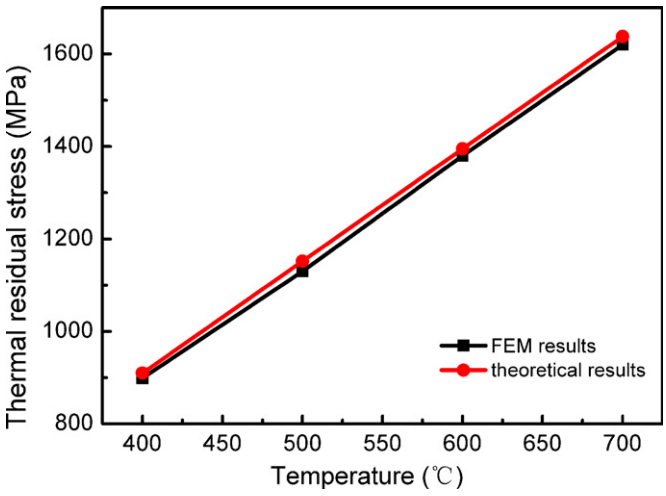

Fig. 4. FEM and theoretical results.

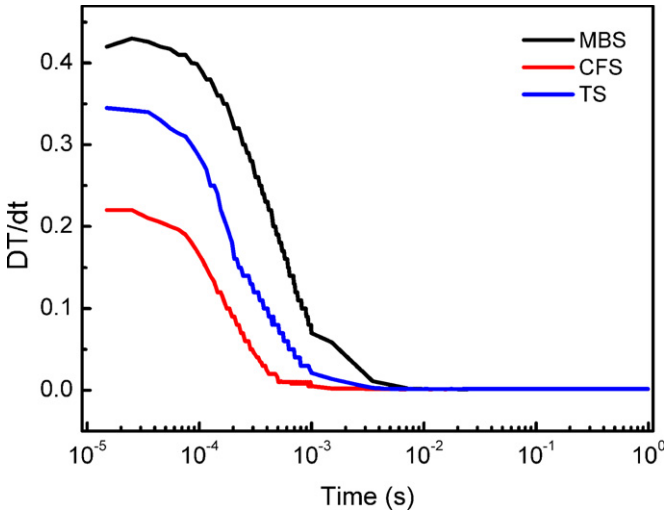

Fig. 5. Temperature variation rate of pyroelectric film as a function of time with different models.

3. Results and discussion

Fig. 5 shows the temperature variation rate (dT/dt) in pyroelectric film with different model structures. An obvious feature is that the values of dT/dt in pyroelectric film decrease with the increasing time, and reach a constant when the time increase up to 10^{-2} s. It also can be seen that the values of dT/dt show a big difference depending on the different models. The different models lead to different heat loss by conduction, and thus, lead to different values of dT/dt. The MBS has the largest values of dT/dt among the three models. So the MBS is further investigated in the following parts.

Fig. 6 shows the temperature variation rate in pyroelectric film versus time with the thickness of silicon substrate as the parameter. The values of dT/dt in pyroelectric film increase with the decreasing thickness of silicon substrate, during 0.005–1 s. This is due to the relatively large thermal conductivity of the

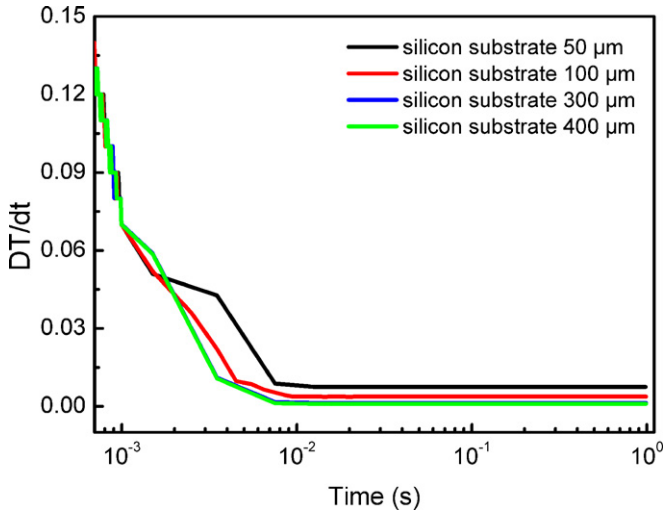

Fig. 6. Temperature variation rate in pyroelectric film versus time with silicon substrate thickness as parameter.

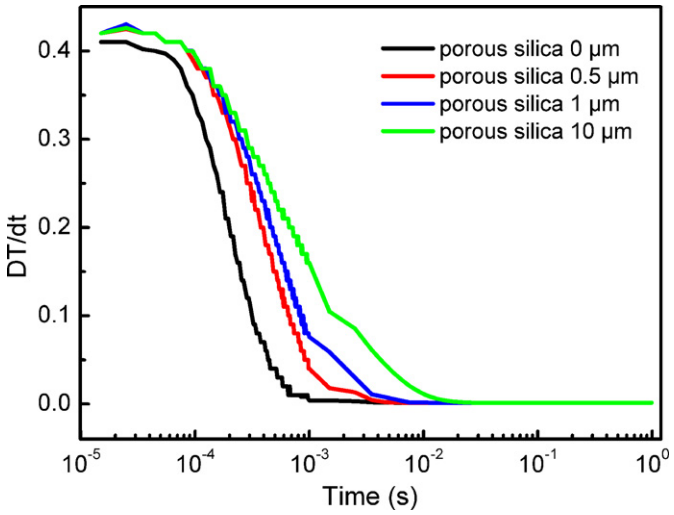

Fig. 7. Time dependence of temperature variation rate in pyroelectric film with different thicknesses of porous silica film.

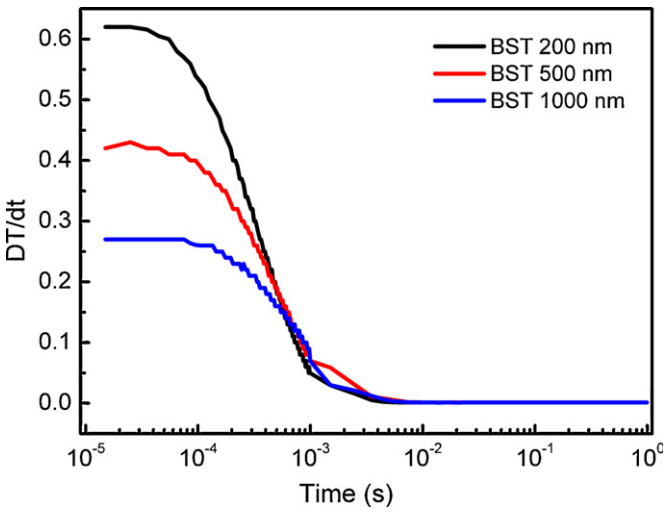

Fig. 8. Temperature variation rate in pyroelectric film with different pyroelectric film thicknesses.

silicon substrate. So in the designing of IR detector, the thickness of silicon substrate should be as thin as possible.

Fig. 7 shows the temperature variation rate in pyroelectric film with different thicknesses of porous silica film. It can been seen from Fig. 7 that without porous silica film as thermal insulator layer, the value of dT/dt in pyroelectric film sharply decreases and reaches the minimum value at 10^{-3} s. With the increasing thickness of porous silica film, the time that the value of dT/dt reaches the minimum moves rightward. It is because the lower thermal conductivity of porous silica, so more heat flow is contributed to increase the value of dT/dt in pyroelectric film in a longer time slice.

The thickness of the pyroelectric film is also a very important factor to the performance of a detector, as shown in Fig. 8. In the case of all other parameters being same, the values of dT/dt in pyroelectric film increase with the decreasing thickness of pyroelectric film. It is believed that the thick pyroelectric film has a relatively bigger thermal capacity, compared with a thin

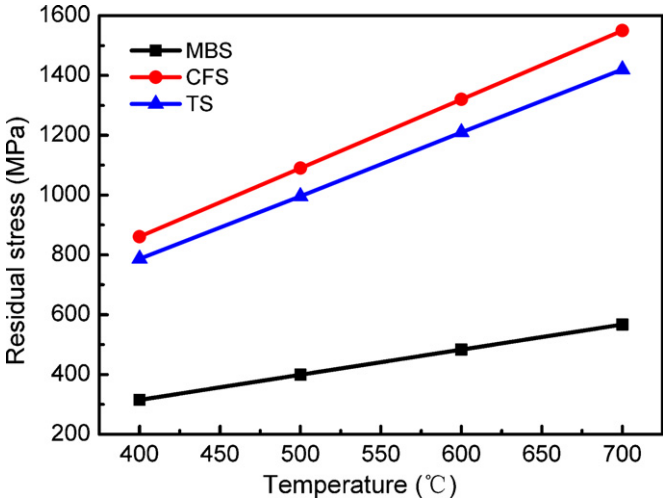

Fig. 9. Thermal residual stresses of the pyroelectric film as a function of annealing temperature with different models.

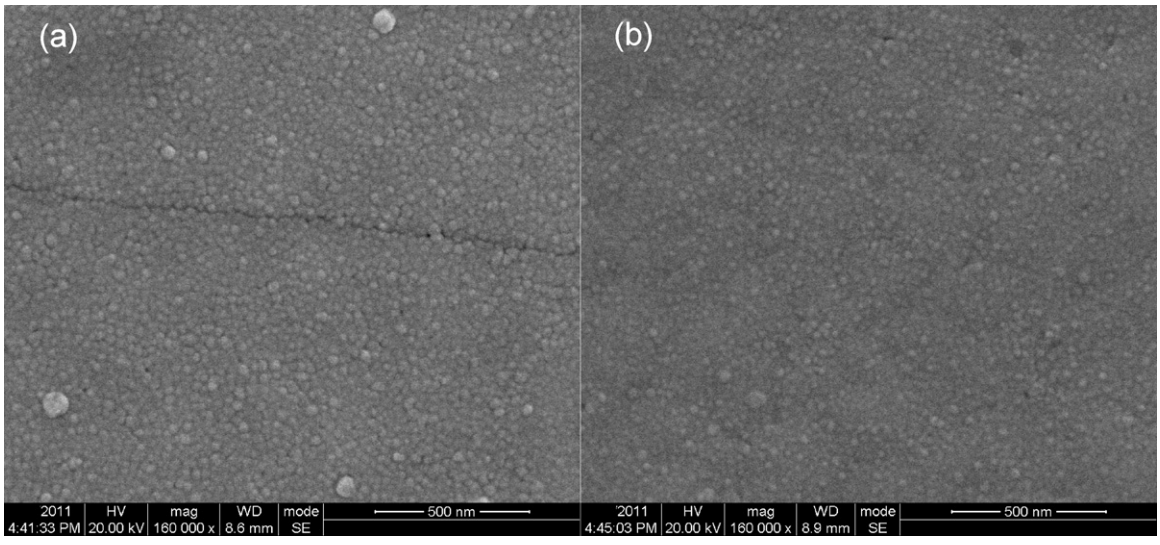

Fig. 10. SEM micrograph of BST film for the CFS annealed at (a) 750 °C and (b) 600 °C.

pyroelectric one. In this sense, the thin film pyroelectric material has its obvious advantage over the pyroelectric bulky one.

The thermal residual stresses in the BST thin film as a function of annealing temperature with different models were shown in Fig. 9. From Fig. 9, it can be seen that the residual stresses increase rapidly with the increasing annealing temperature. The higher the temperature, the larger the temperature difference, so the larger the residual stress that induced by the mismatch of thermal expansion coefficient between different films. The MBS has the lowest residual stress within the three different models. The BST film was prepared by radio frequency magnetron sputtering. The SEM micrograph of BST film for the CFS was shown in Fig. 10. The BST film has a crack when annealed at 750 °C, and is crack-free when annealed at 600 °C.

4. Conclusion

By using the finite element method, temperature field and residual stress of multilayer pyroelectric thin film detector were simulated. The simulation results proved that the MBS has the largest value of dT/dt in pyroelectric film than the other models. The porous silica film obviously reduced the heat loss due to the conduction of heat from the pyroelectric film to the silicon substrate. With the increase of silicon substrate thickness, the response value of dT/dt decreases. The thinner the pyroelectric film, the less the heat capacity, and consequently, the better the performance. The simulation results also showed that when the annealing temperatures increase, the thermal residual stresses increase due to the large temperature difference. The MBS shows the lowest residual stress among the three different models. So, a proper thickness matching of porous silica film, pyroelectric film and silicon substrate, and a proper annealing temperature and designing reasonable structure would gain greatest benefits in improving the properties of multilayer pyroelectric thin film IR detector.

Acknowledgements

The author wish to thank the National Natural Science Foundation of China for sponsoring this project (Nos. u0837605 and 60771016).

References

[1] K. No, C.G. Choi, D.S. Yoon, T.H. Sung, Y.C. Kim, I.S. Jeong, W.J. Lee, Pyroelectric properties of sol–gel derived lanthanum modified lead titanate thin films, Jpn. J. Appl. Phys. 35 (1996) 2731–2733.
[2] R.W. Whatmore, Pyroelectric ceramics and devices for thermal infrared detection and imaging, Ferroelectrics 118 (1991) 241–259.
[3] J.S. Ko, W.g. Liu, W.g. Zhu, B.M. Kwak, Influence of the silicon substrate thickness on the response of thin film pyroelectric detectors, Solid-State Electron. 46 (2002) 1155–1161.
[4] J.G. Wu, J.L. Zhu, D.Q. Xiao, J.G. Zhu, J.Z. Tan, Q.L. Zhang, Preparation and properties of highly (100)-oriented $Pb(Zr_{0.2}Ti_{0.8})O_3$ thin film prepared by rf magnetron sputtering with a PbO_x buffer layer, J. Appl. Phys. 101 (2007) 094107.
[5] J.G. Wu, D.Q. Xiao, J.L. Zhu, J.G. Zhu, J.Z. Tan, Enhanced ferroelectric properties of $(Pb_{0.90}La_{0.10})Ti_{0.975}O_3$ multilayered thin films prepared by RF magnetron sputtering, Appl. Surf. Sci. 253 (2007) 8365–8370.
[6] C.G. Wu, Y.R. Li, J. Zhu, X.Z. Liu, W.L. Zhang, Great enhancement of pyroelectric properties for $Ba_{0.65}Sr_{0.35}TiO_3$ films on Pt–Si substrates by inserting a self-buffered layer, J. Appl. Phys. 105 (2009) 044107.
[7] L. Li, L.Y. Zhang, X. Yao, B. Li, Computer simulation of temperature field of multilayer pyroelectric thin film IR detector, Ceram. Int. 30 (2004) 1847–1850.
[8] K. Morito, T. Suzuki, Effect of internal residual stress on the dielectric properties and microstructure of sputter-deposited polycrystalline (Ba,Sr)-TiO_3 thin films, J. Appl. Phys. 97 (2005) 104107.
[9] J.G. Wu, D.Q. Xiao, J.G. Zhu, Effect of residual stress on the ferroelectric property of $(Pb_{0.90}La_{0.10})Ti_{0.975}O_3$ thin films, J. Appl. Phys. 105 (2009) 056107.
[10] H. Zheng, X.J. Zheng, J.S. Wang, G.C. Yu, Y. Li, S.T. Song, C. Han, Evaluation the effect of aspect ratio for Young's modulus of nanobelt using finite element method, Mater. Des. 32 (2011) 1407–1413.
[11] Y.S. Liu, X.J. Shao, J. Liu, Z.F. Yue, Finite element method and experimental investigation on the residual stress fields and fatigue performance of cold expansion hole, Mater. Des. 31 (2010) 1208–1215.
[12] W. Zhang, X. YAO, X.Q. Wu, Two-dimensional thermal analysis of multilayer pyroelectric thin film infrared detector, Infrared Technol. 26 (2004) 60–63.
[13] J. Zhang, M.W. Cole, S.P. Alpay, Pyroelectric properties of barium strontium titanate films: effect of thermal stresses, J. Appl. Phys. 108 (2010) 054103.
[14] C. Daniel, Harris, Durable 3–5 mm transmitting infrared window materials, Infrared Phys. Technol. 39 (1998) 185–201.
[15] H. Julfikar, R. Mahfujur, C. Brian, M.S.J. Hashmia, Simulation of thermal stress in magnetron sputtered thin coating by finite element analysis, J. Mater. Process Technol. 168 (2005) 36–41.